

A Computational and Experimental Analysis of Ballistic Impact to Sheet Metal Aircraft Structures

Authors:

Matti J. Loikkanen, Boeing Commercial Airplanes
Murat Buyuk, FHWA/NHTSA National Crash Analysis Center,
The George Washington University
Cing-Dao (Steve) Kan, FHWA/NHTSA National Crash Analysis Center,
The George Washington University
Nick Meng, SGI

Correspondence:

Murat Buyuk

(703)726-3616
(703)726-3530
mbuyuk@ncac.gwu.edu

Keywords:

Ballistic impact, finite element analysis, aircraft structures

ABSTRACT

The ballistic resistance of 2024-T3 and 2024-T351 alloy aluminum flat plates to aircraft engine fragments is evaluated experimentally. Gas and powder gun tests are performed to determine the ballistic speed limit of a spherical steel bullet representing the engine fragment with a diameter of 0.5 inch. The rectangular flat aluminum specimens are prepared as 12 x 12 inch and with three different thickness combinations of 1/16", 1/8" and 1/4". A normal impact scenario is considered in terms of the orientation of the specimens to the impacting projectile.

A computational model is constructed using Johnson-Cook (J-C) material model considering the thermo-viscoplastic behavior of the material with an accumulated damage and an equation of state model. The experimental model was implemented in LS-DYNA to simulate impact tests and validate the ballistic limit findings with a comparison for the failure mechanisms. Under these controlled geometries, controlled impact conditions, and characterized materials with well-defined material properties, experimental damage characteristics are used to determine the essential failure parameters in the material model.

INTRODUCTION

In the past three years Boeing has participated with FAA and its partners: Lawrence Livermore Laboratory and The University of California at Berkeley, trying to enhance the safety of commercial aircraft in the case of catastrophic engine failure. The overall purpose of the program has been to develop reliable design tools to analyze the damage from engine rotor burst fragments. The present phase of the study focused on improving the understanding of metal fragments impacting and penetrating Aluminum airframe parts such as wings and fuselage, which are close to the engines. The program was composed of comprehensive ballistic testing of the aircraft material, some theoretical developments and finite element model development and simulation. Boeing's effort focused mainly on developing practical finite element modeling capabilities, which can predict with reasonable accuracy and cost a metal fragment impact including penetration, from jet engine rotor burst on Aluminum structures.

This phase of the FAA study had the following three distinct features:

- High strain rate material testing using the Split Hopkinson Bar test apparatus and other similar methods to derive the Aluminum properties for the J-C material model.
- Ballistic testing of flat Aluminum plates.
- Numerical simulations of the experiments.

The J-C material model was chosen to represent Aluminum target plates, because it is known to accurately represent a wide range of strain rates, it accounts for strain hardening, heat generation in the material, and it can model the damage growth and material failure. FAA sponsored a test program to refine the Aluminum 2024-T3 and T351 flow surface constants and the failure parameters for target plate thickness ranging from 1/16" to 1/4". The strain rate spanned up to 1000 /sec in these tests. The target plates were 12 by 12 inch squared and were mounted on heavy steel frames leaving 10 by 10 inch-squared target area. The projectile was a 0.5 inch-diameter steel sphere. Several shots were fired on each plate thickness so that the ballistic limit and the impact vs. residual velocity plot were accurately defined. Both gas and powder gun were employed in the test. The projectile impact and exit (post-impact) speeds and the target failure pattern were recorded with digital videos and still images.

Reliable ballistic impact computations are still a challenge. Advanced computer software is available and many material models exist to depict the behavior of metals under high-speed impact. However, the material data is often not publicly available or is inaccurate and the modeling methods are not very well defined. In this paper newly refined J-C material data for Al2024-T3 and Al2024-T351 is used and some modeling methods i.e. meshing, contact definitions, etc. are described to simulate the recent FAA ballistic tests. All the work reported here was done with LS-DYNA explicit finite element program in the Lagrangian domain. Short description of the tests is first given and then the modeling techniques are outlined. The finite element simulation results are shown and finally a brief discussion and some explanations are offered.

Experimental Investigations

The ballistic tests were all performed in the University of California, Berkeley (UCB) materials laboratory. The tests with initial velocities below 1000 ft/sec were done with the pneumatic gun, and those over 1000 ft/sec needed a powder gun. The target plate thicknesses were 1/16", 1/8" and 1/4" (i.e. 0.0625, 0.1250 and 0.2500 inch). The plates were cut to 12 by 12 inch size and attached to the one inch wide support frame, thus leaving 10 by 10 inch free target area. The projectile was a 0.5 inch diameter chrome steel sphere. The impact and exit velocities were recorded; the damage to the target and failure mode were measured and photographed. Tests were repeated with all target thicknesses so that good approximation of the ballistic limit and the impact-exit velocity plot were possible. A detailed description of the test setup can be found in literature [1]. The ballistic limit prediction graph for each thickness is plotted in Figure 1.

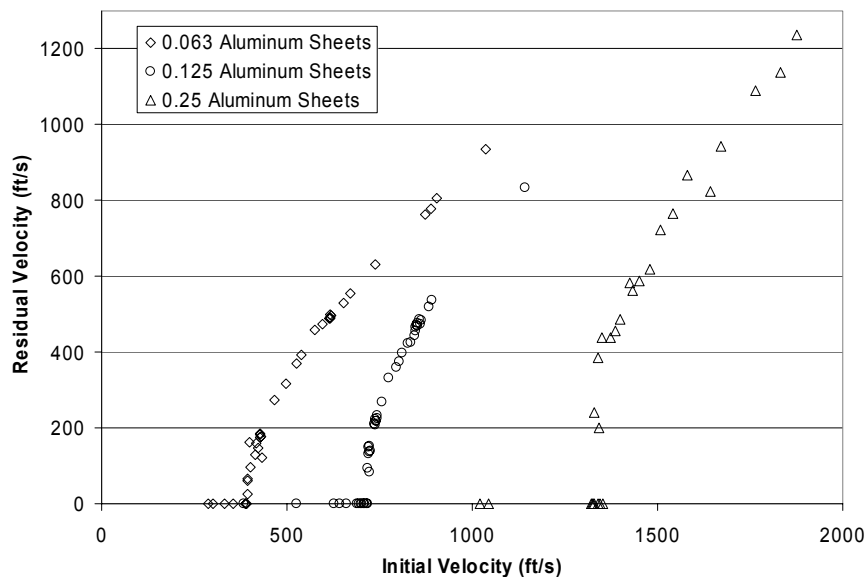


Figure 1. Ballistic limit curve for 2024-T3 Aluminum plates.

Numerical Investigations

Finite Element Model

FE mesh created for the targets and the spherical projectile is shown in Figure 2. The mesh is optimized for stability, accuracy and efficiency of the impact analysis. The circular layers of the armor are divided into three regions in mesh in radial direction and the mesh density is gradually coarsening from inner region

which is the potential impact region to the outer region. Mesh transition between regions are good enough to prevent stress wave reflections from the boundary of regions. The armor and the projectile are meshed with explicit 8-noded hexagonal elements of varying sizes. Maximum aspect ratios of the elements do not exceed five in the mesh. The projectile has a very fine mesh as well. The armor-projectile FE mesh includes a total of 97,000 elements; 4,000 elements for the projectile and 93,000 elements for the 1/16" plate. For the thicker plates the same element size is kept through the thickness. The translational nodal degrees of freedom along the boundary of the armor layers are constrained to prevent any motion. Contact behavior between the projectile and the plate is simulated by using eroding surface-to-surface contact-impact algorithm with SOFT=2 the segment based constraint option.

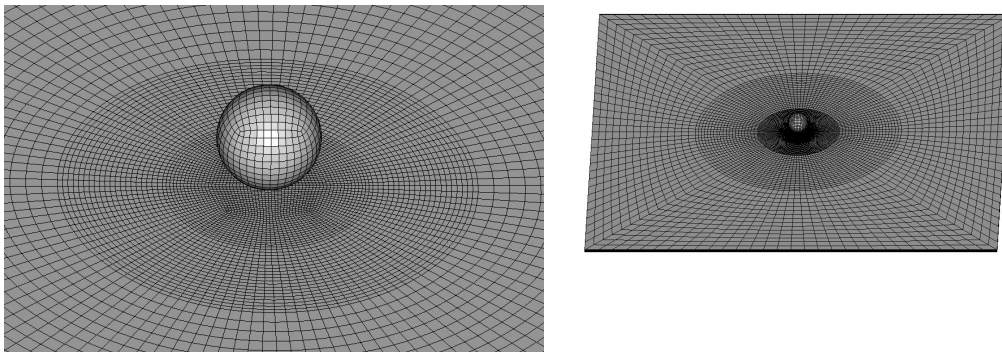


Figure 2. Finite element model of the spherical projectile and planer plate.

Constitutive Models

Plastic kinematic hardening and J-C constitutive models are used to simulate the behavior of steel projectile and aluminum plates respectively. The constitutive model parameters are obtained from four different resources. Two of these sets are published in an FAA report and obtained by Lawrence Livermore National Laboratory (LLNL), where the third one is only a modified version of the second set of parameters obtained at LLNL [2, 3]. The last set of parameters is obtained through the publicly available literature [4, 5].

Plastic Kinematic Hardening Model

Plastic kinematic hardening material model is a strain-rate dependent elastic-plastic model utilized to predict the response of the steel projectile. In this model, strain rate is accounted for using the Cowper-Symonds model which scales the yield stress by the strain rate dependent factor as shown below [6]:

$$\sigma_Y = \left[1 + \left(\frac{\dot{\epsilon}}{C} \right)^{\left(\frac{1}{P} \right)} \right] \sigma_0$$

(1)

where σ_0 is the initial yield stress, $\dot{\epsilon}$ is the strain rate, C and P are the Cowper-Symonds strain rate parameters. If C and P values are equal to zero, strain rate effects are not considered in the formulation. Fracture is simulated by removing elements that reach a user-defined value of equivalent plastic strain (erosion strain). Fracture strain is assumed to be zero for the steel sphere since there is no plastic deformation or failure observed during the experiments. Plastic-kinematic model constants for steel are given in Table 1.

Table 1. Plastic kinematic hardening material constants for steel.

Modulus of Elasticity (psi) E	Density (lb/inch ³) ρ	Poisson Ratio ν	Yield Stress (psi) σ_Y	Tangent Modulus (psi) E_T	Strain Rate Parameters C	P	Failure Strain ϵ_f
3E+7	0.2835992	0.3	68167	0	0	0	0

Johnson-Cook Material Model

Johnson-Cook is a strain-rate and temperature-dependent (adiabatic assumption) viscoplastic model. It is employed to describe the response of 2024-T3 aluminum. The JC model represents the flow stress with an equation of the form [6-8]:

$$\sigma_Y = (A + B\epsilon^n) \left(1 + C \ln \dot{\epsilon}^* \right) (1 - T^{*m})$$

(2)

where σ_Y is the effective stress, ϵ is the effective plastic strain, $\dot{\epsilon}^*$ is the normalized effective plastic strain rate (typically normalized to a strain rate of 1.0 s⁻¹), n is the work hardening exponent and A , B , C and m are constants. The quantity T^* is defined as:

$$T^* = \frac{T - T_{room}}{T_{melt} - T_{room}}$$

(3)

where T_{room} is the room temperature, T_{melt} is the melting temperature and is typically taken as the solidus temperature for an alloy. Fracture in the JC material model is based on a cumulative damage law:

$$D = \sum \frac{\Delta\epsilon}{\epsilon_f}$$

(4)

in which:

$$\epsilon_f = [D_1 + D_2 \exp(D_3 \sigma^*)] \left[1 + D_4 \ln \dot{\epsilon}^* \right] [1 + D_5 T^*]$$

(5)

where $\Delta\epsilon$ is the increment of effective plastic strain during an increment in loading and σ^* is the mean stress normalized by the effective stress. The parameters D_1 , D_2 , D_3 , D_4 and D_5 are fracture constants. Failure of elements is assumed to occur when $D = 1$. The failure strain ϵ_f and thus the accumulation of damage is a function of mean stress, strain rate, and temperature. Failed elements are removed from the FE model. The JC material model was used in conjunction with Mie-Gruneisen equation of state model.

Mie-Gruneisen equation of state

Mie-Gruneisen equation of state model defines the pressure volume relationship in one of two ways, depending on whether the material is compressed or expanded. The Mie-Gruneisen equation of state with cubic shock velocity-particle velocity defines pressure for compressed materials as [6-8]:

$$p = \frac{\rho_0 C_{sp}^2 \mu \left[1 + \left(1 - \frac{\gamma_0}{2} \right) \mu - \frac{a}{2} \mu^2 \right]}{\left[1 - (S_1 - 1)\mu - S_2 \frac{\mu^2}{\mu + 1} - S_3 \frac{\mu^3}{(\mu + 1)^2} \right]} + (\gamma_0 + a\mu)E_{int}$$

(6)

and for expanded materials as:

$$p = \rho_0 C_{sp}^2 \mu + (\gamma_0 + a\mu)E_{int}$$

(7)

where E_{int} is internal energy, C_{sp} is the intercept of the vs-vp curve; $S_1 - S_3$ are the coefficients of the slope of the vs-vp curve, γ_0 is the Gruneisen gamma, a is the first order volume correction to γ_0 , and μ is given as

$$\mu = \frac{\rho}{\rho_0} - 1$$

(8)

The yield surface of the 2024-T3 for four different sets of parameters can be illustrated in Figure 3. As it can be observed the yield surface for LLNL_2 and Modified LLNL_2 are exactly the same, where they have different fracture parameters. LLNL_1 and the parameters obtained through literature are giving a yield surface which is not the same but very close to each other. Damage parameters are also tabulated for these different material model sets in Table 2. Mie-Gruneisen equation of state constants are available in the literature and are not measured for this study [7].

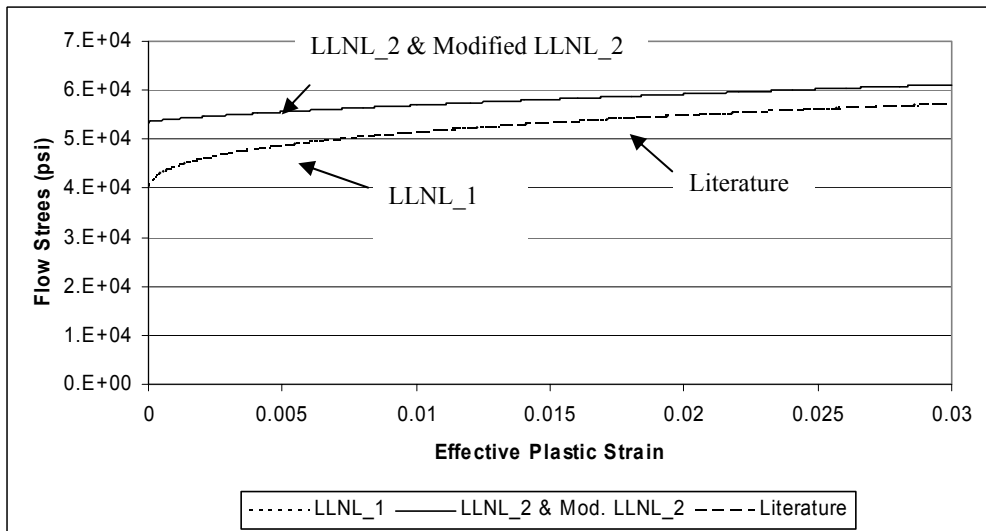


Figure 3. Yield surface for 2024-T3.

Table 2. Damage parameters for material sets.

	LLNL_1	LLNL_2	Modified LLNL_2	Literature
D_1	0.13	0.13	0.31	0.13
D_2	0.13	0.13	0.045	0.13
D_3	-1.5	-1.5	1.7	-1.5

D_4	0.011	0.011	0.005	0.011
D_5	0	0	0	0

Results

To be able to see the trend of the numerical model each and every data point on the experimental graph is simulated. More than four hundred simulations are run on SGI platforms to be able to compare the numerical results with experimental findings. Figure 4, 5 and 6 represent a comparison for 1/16", 1/8 and 1/4" aluminum plates respectively. These graphs compare the simulations results that are obtained by using four different sets of material model parameters, which are LLNL_1, LLNL_2, Modified LLNL_2 and Literature.

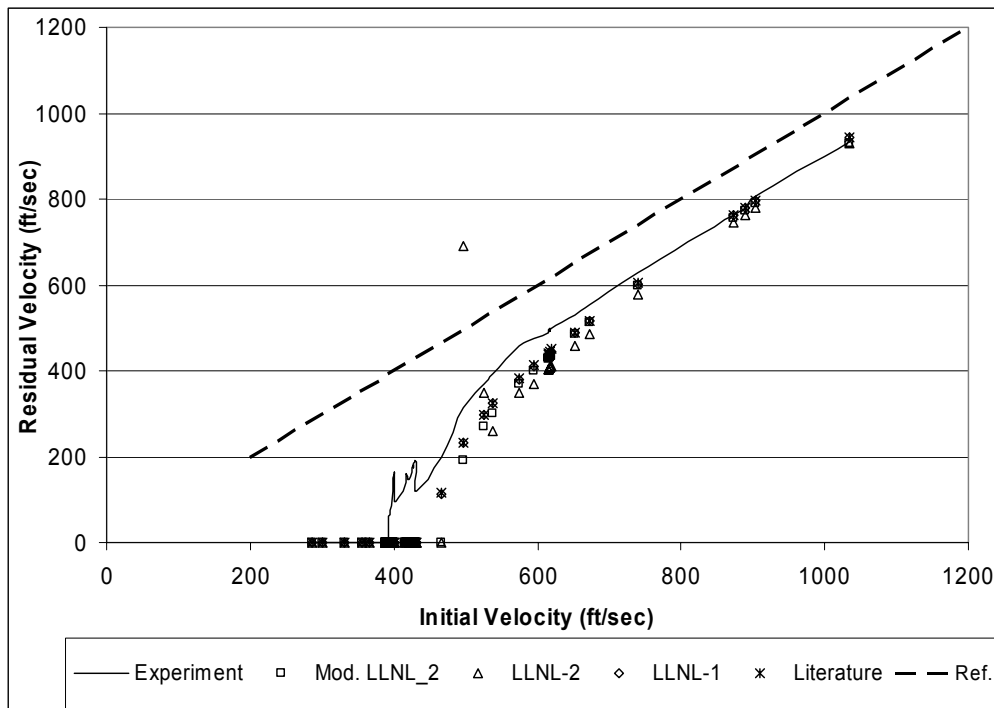


Figure 4. 0.0625" Al 2024-T3 Ballistic Limit Curve

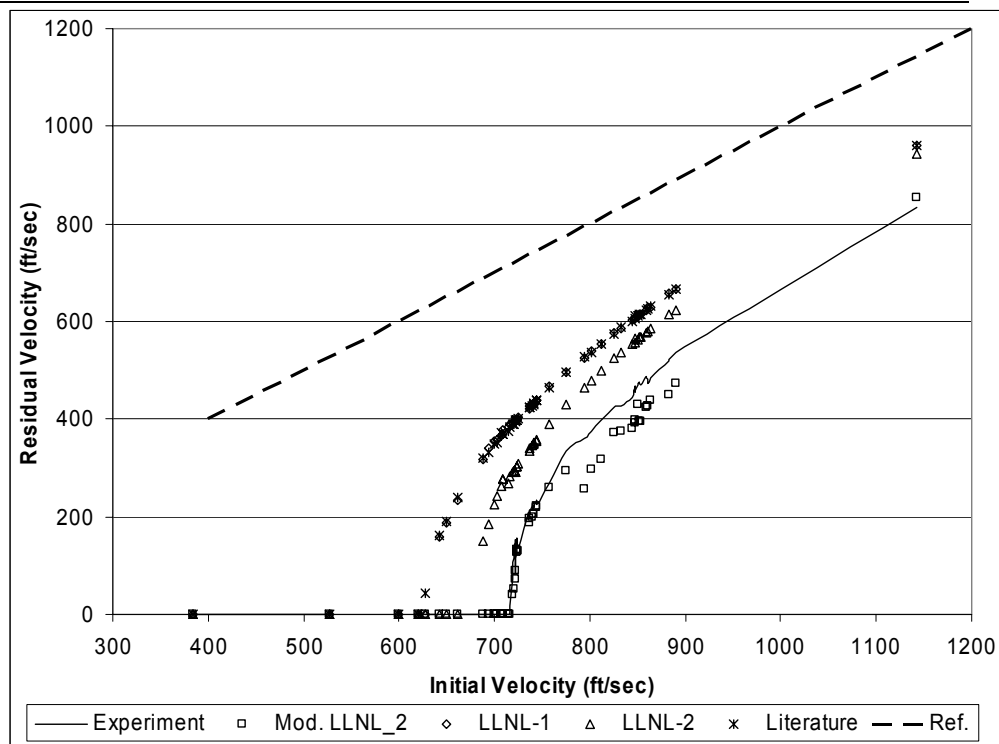


Figure 5. 0.1250" Al 2024-T3 Ballistic Limit Curve

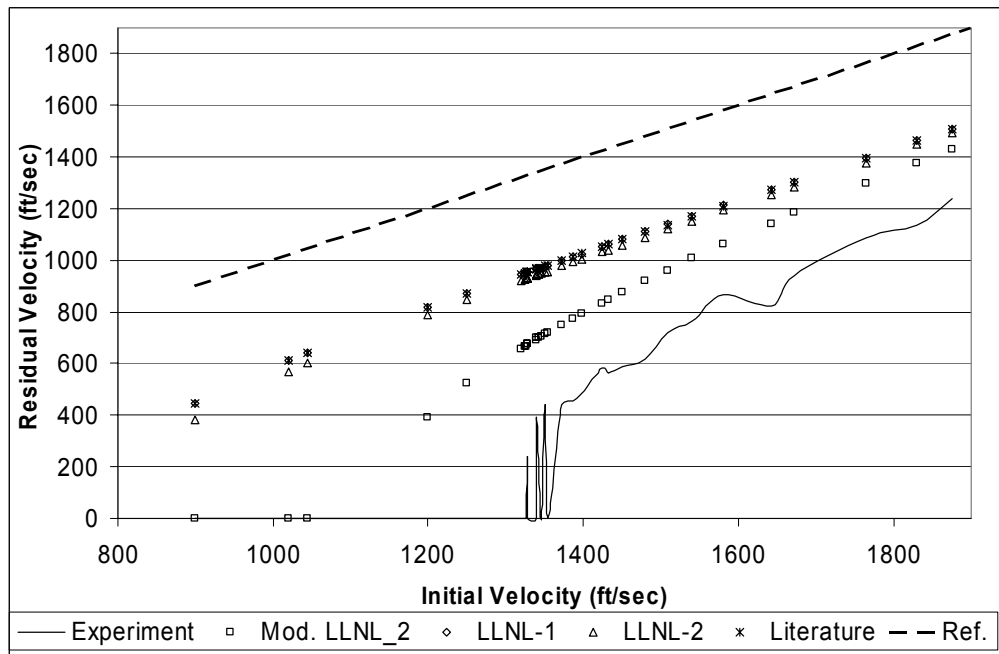


Figure 6. 0.250" Al 2024-T3 Ballistic Limit Curve
Summary and Conclusions

The UCB ballistic tests are simulated with LS-DYNA explicit finite element program. The data shows that the ballistic limit for 1/16 (0.0625) inch plate is

about 400 ft/sec, for 1/8 (0.1250) it is about 700 ft/sec and for ¼ (0.2500) it is about 1350 ft/sec.

The current finite element modeling methods and material data can yield relatively accurate computational results for the plate thickness considered here. The results are somewhat sensitive to the failure mode; bending vs. shear

The LLNL_1 J-C material data gives a better accuracy for thin target plates, which fail in the petaling mode, i.e. bending and tension. The Modified LLNL_2 J-C material data gives the better accuracy for thick target plates, which fail in the plugging mode, i.e. in shear. The Modified LLNL_2 gives better overall accuracy.

References

1. KELLY, SEAN, "THE CHARACTERIZATION OF FAILURE OF COMMON INDUSTRIAL MATERIALS USED IN THE AIRCRAFT INDUSTRY UNDER BALLISTIC IMPACT", MECHANICAL ENGINEERING, MASTERS PAPER, UNIVERSITY OF CALIFORNIA, BERKELEY, MAY 2004.
2. LESUER, DONALD R., "EXPERIMENTAL INVESTIGATIONS OF MATERIAL MODELS FOR TI-6Al-4V TITANIUM AND 2024-T3 ALUMINUM", LAWRENCE LIVERMORE NATIONAL LABORATORY, DOT/FAA/AR-00/25, SEPTEMBER 2000.
3. GOGOLOWSKI, RAYMOND P., MORGAN, BRUCE R., "BALLISTIC EXPERIMENTS WITH TITANIUM AND ALUMINUM TARGETS", LAWRENCE LIVERMORE NATIONAL LABORATORY, DOT/FAA/AR-01/21, APRIL 2001.
4. GORDON R. JOHNSON AND WILLIAM H. COOK, "A CONSTITUTIVE MODEL AND DATA FOR METALS SUBJECT TO LARGE STRAINS, HIGH STRAIN RATES AND HIGH TEMPERATURES", PRESENTED AT THE SEVENTH INTERNATIONAL SYMPOSIUM ON BALLISTICS, THE HAGUE, THE NETHERLANDS, APRIL 1983.
5. JONAS A. ZUKAS, "HIGH VELOCITY IMPACT DYNAMICS", JOHN WILEY, NEW YORK, 1990.
6. HALLQUIST, J.O., "LS-DYNA KEYWORD USER'S MANUEL", LIVERMORE SOFTWARE TECHNOLOGY CORPORATION, LIVERMORE, CA, USA, 2003.
7. KURTARAN H., BUYUK M., ESKANDARIAN A., "DESIGN AUTOMATION OF A LAMINATED ARMOR FOR BEST IMPACT PERFORMANCE USING APPROXIMATE OPTIMIZATION METHOD", INT. JOURNAL OF IMPACT ENGINEERING 29, 397-406, 2003.
8. KURTARAN H., BUYUK M., ESKANDARIAN A., "BALLISTIC IMPACT SIMULATION OF GT MODEL VEHICLE DOOR USING FINITE ELEMENT METHOD", THEORETICAL AND APPLIED FRACTURE MECHANICS, 40, 113-121, 2003.

